

Enhancement of Antiferromagnetic Correlations Induced by Nonmagnetic Impurities: Origin and Predictions for NMR Experiments

Markus Laukamp, George Balster Martins, Claudio Gazza, André L. Malvezzi, and Elbio Dagotto
*National High Magnetic Field Lab and Department of Physics,
 Florida State University, Tallahassee, Florida 32306, USA*

Patricia M. Hansen, Alfredo C. López, and José Riera
Instituto de Física Rosario y Departamento de Física, Avenida Pellegrini 250, 2000 Rosario, Argentina

Spin models that have been proposed to describe dimerized chains, ladders, two dimensional antiferromagnets, and other compounds are here studied when some spins are replaced by spinless vacancies, such as it occurs by *Zn* doping. A small percentage of vacancies rapidly destroys the spin gap, and their presence induces enhanced antiferromagnetic correlations near those vacancies. The study is performed with computational techniques which includes Lanczos, world-line Monte Carlo, and the Density Matrix Renormalization Group methods. Since the phenomenon of enhanced antiferromagnetism is found to occur in several models and cluster geometries, a common simple explanation for its presence may exist. It is argued that the resonating-valence-bond character of the spin correlations at short distances of a large variety of models is responsible for the presence of robust staggered spin correlations near vacancies and lattice edges. The phenomenon takes place regardless of the long distance properties of the ground state, and it is caused by a “pruning” of the available spin singlets in the vicinity of the vacancies. The effect produces a broadening of the low temperature NMR signal for the compounds analyzed here. This broadening should be experimentally observable in the structurally dimerized chain systems $Cu(NO_3)_2 \cdot 2.5H_2O$, $CuWO_4$, $(VO)_2P_2O_7$, and $Sr_{14}Cu_{24}O_{41}$, in ladder materials such as $SrCu_2O_3$, in the spin-Peierls systems $CuGeO_3$ and NaV_2O_5 , and in several others since it is a universal effect common to a wide variety of models and compounds.

I. INTRODUCTION

The theoretical and experimental study of quasi-one dimensional compounds continues attracting considerable attention. Among these materials a large number of systems which can be described by Hamiltonians where the relevant degrees of freedom are localized spins have been studied using a wide variety of techniques. Interesting spin gapped and gapless systems and models have been identified. In particular, compounds with “ladder” structures are currently under much investigation [1]. The excitement surrounding these compounds was originally triggered by theoretical predictions suggesting (i) the existence of a spin gap in the undoped case, and (ii) a transition to a superconducting state upon hole doping. A vast amount of experimental literature has indeed confirmed that ladder materials, such as $SrCu_2O_3$, are gapped [2], and more recently the presence of superconductivity upon hole doping and under high pressure in the ladder compound $Sr_{0.4}Ca_{13.6}Cu_{24}O_{41.84}$ has been reported [3]. Ladders appear to be near ideal systems where theoretical many-body calculations can be carried out with such accuracy that their predictions can be contrasted directly with experiments. In the context of ladders recently some challenging results have been experimentally observed replacing *Cu* by *Zn* (a process which

usually is considered equivalent to adding vacancies to the compound under investigation). In this situation the spin gap of the pure system was observed to decrease very rapidly with *Zn*-doping, and, even more surprisingly, antiferromagnetic order was found to be stabilized by this procedure [4]. Such ordering effect caused by the apparently disordering addition of vacancies is puzzling.

In parallel with the recent excitement in the context of ladder systems, another gapped low-dimensional compound has received much attention. It has been shown that $CuGeO_3$ has a spin-Peierls transition at 14K and at lower temperatures the compound is dimerized, with a finite spin gap. While the addition of mobile carriers to this compound has not been achieved, at least static vacancies can be introduced by the same procedure as in ladders i.e. replacing *Cu* by *Zn*. It is a remarkable experimental result that $Cu_{1-x}Zn_xGeO_3$ was found to have a very similar behavior as *Zn*-doped ladders (up to an overall energy scale) i.e. the original gap is rapidly suppressed and antiferromagnetic order is stabilized after a small percentage of *Zn* is introduced in the system [5].

There are other compounds which present an intrinsic structural dimerization not caused by the coupling of spins and phonons. $Cu(NO_3)_2 \cdot 2.5H_2O$ [6] and $CuWO_4$ [7], provide examples of this behavior. More recently it has been shown that $(VO)_2P_2O_7$, originally

considered a two-leg spin ladder along the a direction, is actually better described by alternating spin chains running along the b direction [8]. In addition, the compound $Sr_{14}Cu_{24}O_{41}$ mentioned above contains both two-leg ladders and structurally modulated CuO_2 chains [9].

These experimental results have generated a large body of theoretical work. Using a variety of many-body techniques and models, the issue of the rapid collapse of the spin-gap upon the addition of vacancies in both ladders and dimerized chains have been explained by the appearance of localized spin $1/2$ states near the doped vacancies [10–12]. For a very Zn -dilute system the average distance between these states is large and, thus, the spins are weakly interacting. Calculations have shown that these localized states form a low energy band in the spectrum which appear inside the original spin gap [10,11]. Predictions for inelastic neutron scattering (INS) experiment revealed that for doped samples while a large weight should still exist near a frequency ω corresponding to the original gap, extra weight growing proportional to x should also be observed inside the gap [10]. The results of recent INS experiments on doped $CuGeO_3$ are compatible with this prediction [13]. Also Raman scattering results for in-chain and off-chain substitutions in $CuGeO_3$ has been interpreted as signaling the presence of low energy excitations inside the original gap, in agreement with the theoretical studies [14]. In addition, very recent EPR experiments carried out for $CuGeO_3$ with up to 5% Zn doping have revealed structure that is also compatible with the presence of localized spins induced by vacancies [15]. It is interesting to note that while all these experimental techniques have enough resolution in energy to separate features that smoothly evolve from the pure sample from those that are induced by doping, measurements of the static susceptibility may simply suggest the collapse of the gap rapidly with Zn -doping since this quantity at low temperature is dominated by the low energy states. This was precisely the conclusion of the first papers on Zn doped ladders and dimerized chains [5,4]. Then, the experimental results currently available appear compatible among themselves and the presence of in-gap states is very likely. Thus, currently a consistent scenario exists that could explain the early reports of an apparent drastic reduction of the spin-gap upon the addition of vacancies. This scenario relies on spin $1/2$ states induced near vacancies. Note that these spins will start interacting as the vacancy concentration grows, thus they can be considered as “free” only at very small doping.

On the other hand, the appearance of enlarged antiferromagnetic (AF) correlations upon Zn doping has been more challenging to explain. Numerical calculations applied to dimerized systems and ladders have indeed found that AF enhancement is a property of the spin models used to describe their behavior [10,11], but an intuitive explanation is difficult to find. It is interesting to note that in other contexts similar phenomena have been observed before. For instance, staggered spin correlations are amplified near vacancies in $S = 1$ Heisen-

berg chains [16], presumably caused by the presence of localized $S = 1/2$ states in its vicinity. The $S = 1/2$ Heisenberg model also has a staggered spin structure which is enhanced near the edges of open chains, according to boundary conformal field theory and Monte Carlo simulations [17]. Finally, in the two dimensional (2D) Heisenberg model studies using a 4×4 lattice and spin-wave techniques detected the presence of staggered order enhancement in the immediate vicinity of a vacancy [18].

All these results have been studied mostly independently of each other in the literature. However, recently a simple explanation for the AF enhancement has been proposed [19] using the so-called “pruned” Resonating-Valence-Bond (RVB) picture [20] which can be summarized as follows: at short distances the physics of spin chains is dominated by spin singlet formation. For an undoped system a given spin spends roughly half its time forming a singlet with spin partners at both its right and left. However, if an impurity is located next to the spin under consideration only one direction is now available and this spin attempts to form singlets with its only neighbor more strongly than for the undoped case. Numerical and variational results support this picture [19].

The purpose of the present paper is twofold: (i) first, the ideas introduced in the previous publication Ref. [19] by some of the present authors are here expanded and the computational results are discussed in detail. Some new results for spin correlations are provided, and the generality of the phenomenon of AF enhancement upon Zn -doping is emphasized. (ii) Second, the study of experimentally observable consequences of the AF enhancement, specially for NMR spectra, is discussed in this paper for a variety of models with special emphasis on dimerized chains. It is concluded that the anomalous broadening of the main NMR signal as the temperature is reduced as predicted by Eggert and Affleck [17] for compounds represented by the unfrustrated undimerized $S = 1/2$ Heisenberg model will appear also in other compounds with only small modifications. The techniques mainly used throughout the paper are the Lanczos [21] and Density Matrix Renormalization Group (DMRG) [22] methods, but some results at finite temperature using the world-line Monte Carlo technique will also be presented. The physics discussed here is mostly caused by short distance effects, and thus finite size problems are not expected to affect severely the results and conclusions presented here.

II. EQUAL-TIME SPIN-SPIN CORRELATIONS

In this section numerical results are presented which illustrate the existence of enhanced staggered spin-spin correlations near vacancies for a variety of spin models and cluster geometries. These results suggest that the effect is quite general and caused mainly by short distance physics, which makes it independent of the subtle prop-

erties of the ground state at large distances (i.e. gapped vs gapless spin spectrum).

A. $S = 1/2$ Heisenberg Model With and Without Frustration

The enhancement of staggered spin correlations upon the introduction of vacancies appears clearly in the case of the $S = 1/2$ Heisenberg model defined on a 1D lattice, as previously discussed in the literature [17]. Fig.1 shows results obtained using the DMRG technique [22] on a chain of 128 sites measuring the staggered spin-spin correlation $C_S(i, j) = \langle \mathbf{S}_i \cdot \mathbf{S}_j \rangle (-1)^{i+j}$, where $\langle \dots \rangle$ denotes the expectation value in the ground state and the rest of the notation is standard. The largest change between the correlations at the center of the chain (bulk) compared against those near the edge (which simulates a Zn -impurity) occurs at distance 1, i.e. the correlation among the first two spins next to the vacancy is about 48% larger than for a couple of nearest-neighbor spins located far from that vacancy. The value obtained here for $C_S(1, 2) = 0.652$ is in excellent agreement with recent Bethe Ansatz calculations on open spin chains [23] that reported $C_S(1, 2) = 0.6515$. The enhancement can also

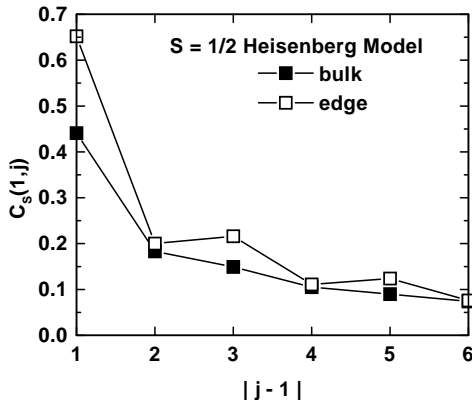


FIG. 1. $C_S(1, j)$ for the spin $1/2$ Heisenberg model without frustration or dimerization (using the DMRG method on a chain with 128 sites). The open (full) squares are results obtained locating site “1” next to the edge (at the center of the chain).

be observed at larger distances specially when $|i - j|$ is odd (note the “zig-zag” pattern of Fig.1 for “edge” results), and it slowly decays with distance. If the results are transformed to momentum space, the real space enhancement translates into an increase of the spin structure factor $S(q = \pi)$ (as remarked in Ref. [17]).

Adding frustration in the form of a coupling $J_2 > 0$ between spins located at a distance of two lattice spacings does not change qualitatively the effect observed in Fig.1.

The Hamiltonian is now

$$H_{J_1 - J_2} = J_1 \sum_i \mathbf{S}_i \cdot \mathbf{S}_{i+1} + J_2 \sum_i \mathbf{S}_i \cdot \mathbf{S}_{i+2}, \quad (1)$$

in the standard notation. Fig.2 contains results for the case $J_2/J_1 = 0.3$ which corresponds to a coupling where the ground state has a small but finite spin gap in the spectrum. The spin correlations obtained with both the Lanczos and DMRG techniques provide very similar results. The main effect of frustration is to reduce the amplitude of these spin correlations at intermediate and large distances (and it suppresses the zig-zag pattern of the unfrustrated case), but at least at distance 1 the enhancement is still clearly present.

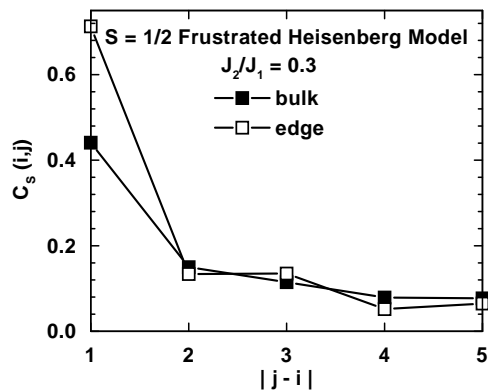


FIG. 2. $C_S(i, j)$ for the $J_1 - J_2$ Heisenberg model at $J_2/J_1 = 0.3$ (using the Lanczos method on a chain with 14 sites). The open squares are results obtained locating site “i” next to the edge using open boundary conditions (OBC). The full squares denote results using periodic boundary conditions (PBC).

B. Dimerized Chains

The recent considerable effort devoted to the experimental and theoretical study of dimerized quasi-one dimensional compounds motivated us to investigate the enhancement of AF near vacancies for a simple dimerized $J_1 - J_2 - \delta$ model defined as

$$H = J_1 \sum_i (1 - (-1)^i \delta) \mathbf{S}_i \cdot \mathbf{S}_{i+1} + J_2 \sum_i \mathbf{S}_i \cdot \mathbf{S}_{i+2}, \quad (2)$$

where the dimensionless parameter δ creates “strong” and “weak” links for the nearest-neighbor spin exchange. The rest of the notation is standard. The presence of a finite J_2 is added for completeness since some dimerized compounds seem to have a sizable next-nearest-neighbors spin-spin interaction [24]. Note that the use of Hamiltonian Eq.(2) to study the influence of Zn -doping assumes that the pattern of strong and weak links does not change upon doping. While this assumption is reasonable for

the many structurally dimerized systems described in the Introduction, it is questionable for spin-Peierls systems where phonons are dynamical variables that could alter the dimerization pattern. This issue will be discussed later in the paper. The calculations using Eq.(2) are very similar to those for the undimerized spin models of the previous section. The Lanczos results corresponding to couplings expected to be realistic such as $\delta = 0.03$ and $J_2/J_1 = 0.2$ are shown in Fig.3 (DMRG results are not shown since they are very similar). Once again, a large enhancement of correlations is observed at short distances, and here the zig-zag pattern of the gapless case is still clearly visible. It is interesting to observe that at distance 1 (i.e. studying $C_S(i, i + 1)$) the enhancement obtained comparing results at the edge and in the bulk is larger than in the undimerized case. To understand this effect consider three consecutive spins labelled as “0”, “1”, and “2” on the chain, and assume that the link between “0” and “1” is strong (and, then, that the link “1” with “2” is weak). Without vacancies in the neighborhood the correlation between spins “1” and “2” is small since they share a weak link. However, now assume that the spin “0” is removed (a vacancy is added). In this case spin “1” has lost its partner to form singlets with, and, as a consequence, a free $S = 1/2$ near the end is created (as discussed recently in Ref. [10]). This spin strongly attempts to form a singlet with the only nearest neighbor spin available which is “2”, enhancing substantially their correlation. If the first pair of spins next to the vacancy

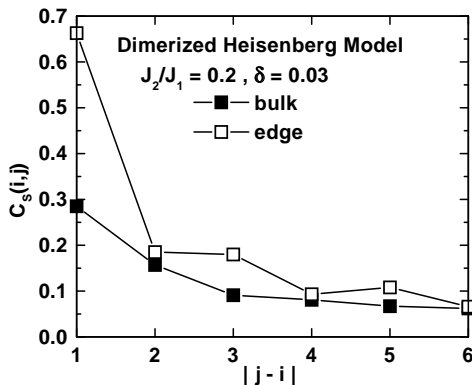


FIG. 3. $C_S(i, j)$ for the $J_1 - J_2 - \delta$ Heisenberg model at $J_2/J_1 = 0.2$ and $\delta = 0.03$ (using the Lanczos method on a chain with 14 sites). The open squares are results obtained locating site “i” next to the edge using OBC. The full squares denote results using PBC.

were linked by a strong bond rather than weak, then the enhancement would not be as dramatic. In other words, the free spin induced by Zn -doping on a dimerized chain is located either at the left or right of the vacancy, and the place where the AF enhancement occurs is correlated with the location of that free spin.

C. Ladders

The existence of a vacancy-induced enhancement of antiferromagnetic spin correlations is not restricted to chains. As shown below the effect also appears on ladders and planes. As remarked in the introduction this is of particular importance since recent experimental results showed that upon Zn -doping ladder compounds develop strong AF correlations at low temperatures [4]. Consider a $S = 1/2$ Heisenberg model defined on a 2-leg ladder. Fig.4a shows $C_S(i, j)$ for a 2×32 cluster with DMRG results obtained both along the leg where the impurity is located and also along the opposite leg. The result shows that $C_S(i, j)$ is specially enhanced for “same leg” correlations. This enhancement at distance 1, i.e. considering $C_S(i, i + 1)$, is about 22% which is smaller than for a spin chain.

Fig.4b contains results for the case of a ladder where the rung and leg couplings (J_\perp and J , respectively) are selected such that the chains are not as strongly coupled with each other as for the case of an isotropic ladder. No vacancy is introduced here but simply the correlations are measured with open and periodic boundary conditions, starting in the former from the edge of the ladder. In this situation the spin correlations resemble qualitatively the results found before for the $S = 1/2$ Heisenberg chain including the zig-zag pattern in the enhancement.

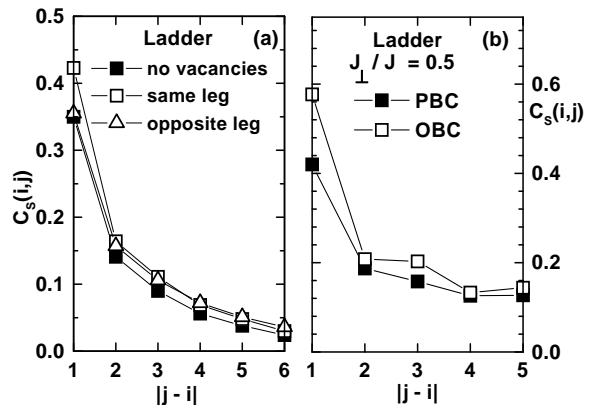


FIG. 4. (a) $C_S(i, j)$ for a two-leg ladder calculated with DMRG on a 2×32 cluster. Open squares (triangles) denote spin correlations along the same (opposite) leg where the vacancy is located, with a starting site i next to the vacancy (which itself is at the center of the cluster). Full squares are results without vacancies obtained in the bulk of the cluster; (b) $C_S(i, j)$ for a two-leg ladder calculated with the Lanczos method on a 2×10 cluster at coupling $J_\perp/J = 0.5$. Full squares are results with PBC. Open squares are results with OBC and correlations measured from the edge of the cluster.

Studying a variety of ratios J_\perp/J it was observed that the correlations at short distance smoothly interpolate between those of decoupled chains ($J_\perp/J = 0$) and the isotropic limit ($J_\perp/J = 1$). This suggests that the effect

is general and does not depend on the gapped vs gapless character of the ground state, in agreement with the conclusions from the study of the $J_1 - J_2$ chain (only the size of the disturbance is a function of the long distance properties of the Hamiltonian under investigation).

D. Two Dimensions

The existence of enhanced spin-spin correlations due to the presence of a vacancy is not restricted to one dimensional systems. A similar effect occurs also in the two dimensional (2D) Heisenberg model, as previously reported in Ref. [18] for the unfrustrated case. Fig.5a-b shows the spin-spin correlations calculated on a tilted $\sqrt{26} \times \sqrt{26}$ Heisenberg cluster with and without a vacancy, and including a frustrating coupling across the plaquette diagonals of strength J_2 (with J_1 being the nearest-neighbor coupling). Results for a $\sqrt{20} \times \sqrt{20}$ cluster are qualitatively similar. The first site i in the correlation is next to the vacancy, and j runs over neighbors at distance 1, $\sqrt{2}$, 2, and $\sqrt{5}$ away from i . Fig.5a-b show that the enhancement effect is mostly restricted to distance 1. In the unfrustrated case $J_2/J_1 = 0.0$, the change of the correlation for the special case $|i - j| = 1$, denoted by Δ_1 , with and without the impurity is about 11%.

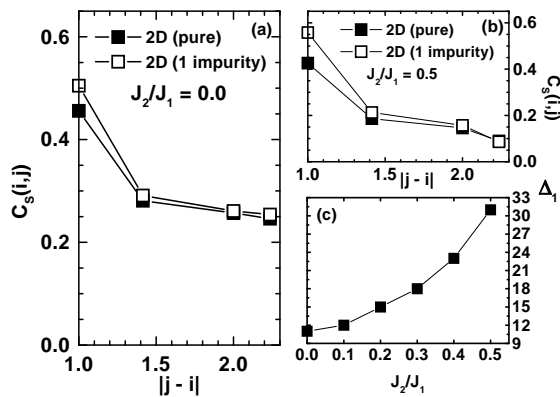


FIG. 5. (a) $C_S(i, j)$ on a $\sqrt{26} \times \sqrt{26}$ tilted square cluster calculated with exact diagonalization. Open (full) squares denote results with (without) a vacancy. i is the site next to the vacancy if present. Correlations at distances 1, $\sqrt{2}$, 2 and $\sqrt{5}$ away from site i are shown; (b) Same as (a) but introducing frustration using the coupling $J_2/J_1 = 0.5$; (c) Relative enhancement Δ_1 (in %) of the spin-spin correlation at distance of one lattice spacing (between a site next to the vacancy and its neighbor in the direction away from the vacancy) vs. J_2/J_1 .

On the other hand, at $J_2/J_1 = 0.5$ i.e. in a situation where the frustration is strong enough to melt the antiferromagnetic order (but not strong enough to make the system collinear [25]) Δ_1 is about 31% (Fig.5c shows Δ_1 vs J_2/J_1 for other couplings). It is clear that the

enhancement occurs more easily when the tendency to form an antiferromagnetic ground state is suppressed i.e. when the disordering effects are strong. However, once again the existence of the effect itself does not seem much related with the long distance ground state properties of the system. It is likely that the enhancement is caused by the behavior at *short* distance which likely is similar to frustrated and unfrustrated Heisenberg models.

E. 1D $S = 1$ Heisenberg Model

The results described in this section are not restricted to $S = 1/2$ systems but the AF enhancement also appears in models with a higher spin, as shown below. This can be understood intuitively recalling that at zero temperature a classical spin system ($S \rightarrow \infty$) is antiferromagnetically ordered even on a chain with open boundary conditions (OBC). Then, while in the $S = 1/2$ case there is a clear AF enhancement, for $S = \infty$ the effect is not present in the ground state. As a consequence, it is reasonable to expect that for spins such as 1 the spin-spin correlation enhancement should roughly interpolate between $S = 1/2$ and ∞ . Fig.6a shows $C_S(i, j)$ for a 1D $S = 1$ Heisenberg model. This clear AF enhancement observed in Fig.6 was extensively discussed in previous literature and it was attributed to $S = 1/2$ states localized near

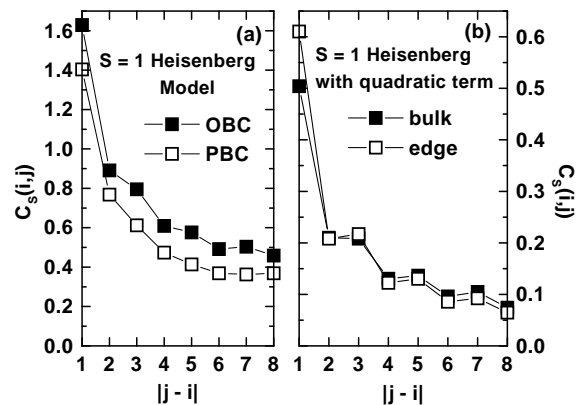


FIG. 6. $C_S(i, j)$ for the 1D $S = 1$ Heisenberg model obtained with the DMRG technique on a chain with 32 sites and keeping $m = 27$ states in the iterations. The notation is as in previous figures. (a) denotes results for the pure Heisenberg model, while (b) has results adding a $-J \sum_i (\mathbf{S}_i \cdot \mathbf{S}_{i+1})^2$ term to the Hamiltonian (inducing a gapless ground state).

the edges [16]. Although the relative enhancement at distance 1 is smaller than for the case $S = 1/2$, it is remarkable that the effect extends over a surprisingly large distance. Fig.6b shows results adding a term $-J \sum_i (\mathbf{S}_i \cdot \mathbf{S}_{i+1})^2$ to the Heisenberg model. This particular addition renders the ground state gapless [26]. The results for the spin correlations show that in this case there is an enhancement in the correlation which has a

staggered pattern very similar to the one observed for the $S = 1/2$ unfrustrated model (Fig.1). This example shows that qualitatively the effect discussed here will likely appear for any finite S spin chain and for both gapped and gapless models (although its actual intensity depends on the details of the ground state under investigation).

III. “PRUNED” RVB BASIS

The results shown in the previous section suggest that a universal mechanism may be at work since a variety of models and cluster geometries present the same phenomenon of enhanced antiferromagnetism near vacancies. In this section a tentative explanation for this effect is given in terms of the Resonating-Valence-Bond states in its short-range version i.e. with states obtained from a covering of the lattice with short dimers [27]. The use of these states to explain the *short* distance phenomenon studied here can be justified even if globally such short-range RVB states do not properly represent the ground state properties of the model under consideration. A typical example is given by the 2D antiferromagnetic Heisenberg model: in this case it is well-known that at zero temperature the model is gapless, with long-range order, and that it cannot be represented by a combination of short-range RVB states since they have a spin gap. However, numerical studies have shown [28] that the exact ground states of *finite* clusters actually have a large overlap with the short-range RVB state for the same cluster. This suggests that at short distances even an asymptotically ordered system such as a 2D Heisenberg model can be approximated by a superposition of spin singlets. Of course, to obtain the proper long-range behavior in the bulk spin singlets linking sites at large distances are needed.

Based on this discussion the following scenario is proposed [19]. Consider Fig.7a,b where a couple of configurations with short spin singlets are represented. These spin arrangements are expected to be important for a variety of spin models in 1D, and in particular it is the exact ground state for the frustrated Heisenberg model with $J_2/J_1 = 0.5$ [29]. Consider now a vacancy introduced at the site labeled as “0” and let us study what happens with the configuration shown in Fig.7b: in this case a free spin is generated next to the vacancy (schematically shown in Fig.7c). This free spin will tend to couple strongly with its neighbor and, thus, the configuration Fig.7d will have a high probability as the system evolves in time. Eventually, the free spin can move some distance away from the vacancy following the same procedure and configuration Fig.7e is reached. For the case of the $S = 1/2$ Heisenberg model this “free” spin is not bounded to the vacancy. This is a manifestation of the well-known effect of spin-charge separation in the case of the $t - J$ model in one dimension for the special case of static holes (in the rest of the text when “spin-

charge separation” is invoked it must be understood in this framework). For other models such as the 2-leg ladders or dimerized systems the free spin can be localized

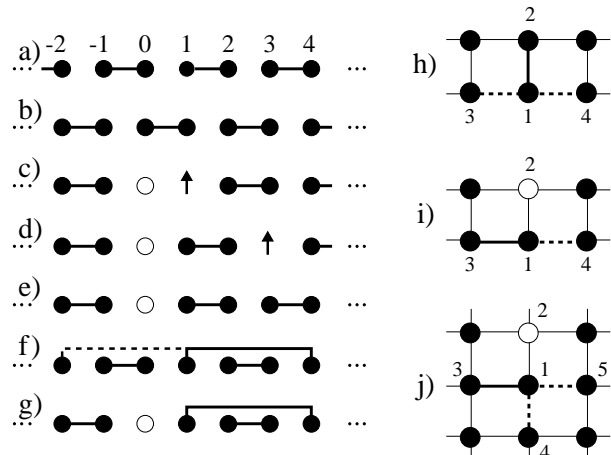


FIG. 7. (a)-(g) Examples of spin singlets relevant for the “pruned” RVB scenario proposed as an explanation for the numerical results; (h)-(j) Spin singlets relevant for ladders and planes. See text for details. (taken from Ref. [19]).

in a finite region near the vacancy [30,10]. But as long as the size of this spin-vacancy bound state is more than three or four lattice spacings the reasoning that led to Fig.7a-e can be applied. The conclusion is that the spin next to the vacancy (spin “1”) forms a singlet with only one partner after spin “0” is removed simply because there is only one partner available, while without vacancy doping the spin at “1” would spend equal amounts of time coupled with spin partners at both its right and left. This effect naturally causes an enhancement of the correlation $\langle \mathbf{S}_1 \cdot \mathbf{S}_2 \rangle$ due to the introduction of the vacancy. Zn doping effectively *prunes* the set of possible RVB spin configurations from 2 down to 1. Spin “1” no longer resonates but its partner is fixed by geometry.

The same reasoning applies if singlets longer than one lattice spacing are considered. Fig.7f illustrates the situation where the spin “1” is coupled with “4” through a singlet of length 3. In this case by symmetry arguments in the wave function a singlet between “1” and “-2” will exist carrying equal weight. However, once again by cutting the chain introducing a vacancy at “0” only one possibility remains as in the case of the short spin singlets, and the correlation between “1” and “4” is enhanced (Fig.7g). The same reasoning can be repeated for longer singlets, although their importance decays with distance and eventually results close to those obtained far from the edge should be obtained when $C_S(1, j)$ is calculated.

The argument presented here leads to the prediction that the AF enhancement should be maximized in 1D. The idea is illustrated in Fig.7h for the case of a 2-leg ladder geometry: if a vacancy is introduced at a given site, the spin next to it along the same rung now has only 2 possible spin partners to form singlets while be-

fore it had 3. Thus, the spin correlation between the spin under study and its 2 neighbors will be enhanced [31]. Repeating the same argument for a 2D system, the ratio of partners before and after the vacancy is 4 and 3, respectively. In general for an arbitrary dimension D , the ratio is $(2 \times D)/(2 \times D - 1)$ which tends to 1 as D grows. Then, one dimensional systems are the best candidates to present a substantial enhancement of correlations due to vacancies. The previous numerical results in 2D clusters showing a spin enhancement smaller than in 1D supports this reasoning.

These ideas can be further tested using RVB-like variational wave functions on small clusters. Using the notation (ij) to denote a singlet between the spins at sites i and j , and $[i, j]_\sigma$ for a triplet between the same two spins with total projection $\sigma = 1, 0, -1$, the proposed state is

$$|RVB\rangle = |(12)(34)(56)(78)\rangle + \alpha(|(14)(23)(56)(78)\rangle + |(12)(36)(45)(78)\rangle + |(12)(34)(58)(67)\rangle) + \sum_{\sigma, \sigma'} \beta_{\sigma, \sigma'} (|[13]_\sigma[24]_{\sigma'}(56)(78)\rangle + |(12)[35]_\sigma[46]_{\sigma'}(78)\rangle + |(12)(34)[57]_\sigma[68]_{\sigma'}\rangle), \quad (3)$$

where the set $\{\sigma, \sigma'\}$ takes the values $(1, -1)$, $(-1, 1)$, and $(0, 0)$, and $\beta_{1, -1} = \beta_{-1, 1}$ by symmetry. This state is more general than the discussion presented before since it also contains spin triplets that are needed to quantitatively reproduce the spin correlations for the clusters studied. The concept of “pruned” RVB basis can be easily extended to include spin triplets.

Results are shown in Fig.8. Short chains with OBC are considered to simulate the effect of vacancies.

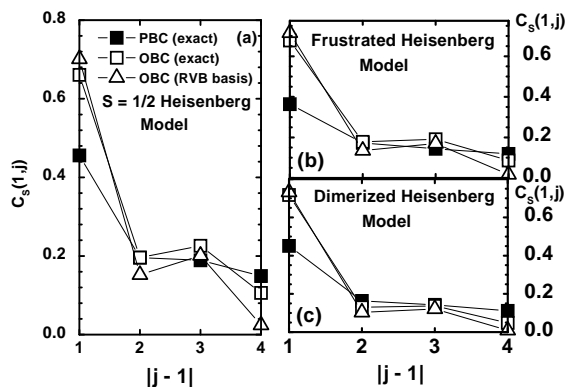


FIG. 8. Staggered spin correlations calculated using RVB variational states (see text) on an 8 site chain with OBC, contrasted against exact results with both OBC and PBC. (a) corresponds to the $S = 1/2$ Heisenberg model; (b) frustrated $J_1 - J_2$ model with $J_2/J_1 = 0.3$; and (c) dimerized $J_1 - J_2 - \delta$ model with $J_2/J_1 = 0.2$ and $\delta = 0.03$.

For the frustrated and unfrustrated $S = 1/2$ Heisenberg model, as well as the dimerized chain, the variational results are very close to those obtained exactly, and both

differ from the correlations for the same lattice size but using PBC where there are no edge effects. The variational state gives remarkably accurate results at distance 1, and since it is dominated by the configuration with the shortest spin singlets it naturally reproduces the zig-zag pattern of some correlations at larger distances. Then, these results suggest that the simple picture presented in this section is robust and the antiferromagnetic enhancement is caused by a pruning of the set of short-range RVB states that describe the short distance behavior of the spin correlations for a variety of spin models.

IV. INFLUENCE OF COULOMBIC INTERACTIONS AND DENSITY

The spin models analyzed thus far can be considered as the strong Coulomb coupling limit of suitable chosen electronic models. In particular, the $S = 1/2$ Heisenberg model is recovered from the one band Hubbard model with nearest-neighbor hopping at large U/t . Then, it is interesting to analyze the enhancement of AF spin correlations discussed in this paper when U/t is varied, and also as a function of the electronic density $\langle n \rangle$ away from half-filling [32]. Fig.9 shows results for the Hubbard model at $U/t = 10, 4$ and 0 , and $\langle n \rangle = 1.0$ (half-filling) as representative of the strong, intermediate, and weak coupling regimes, respectively (note that the bandwidth is $W = 4t$ in 1D).

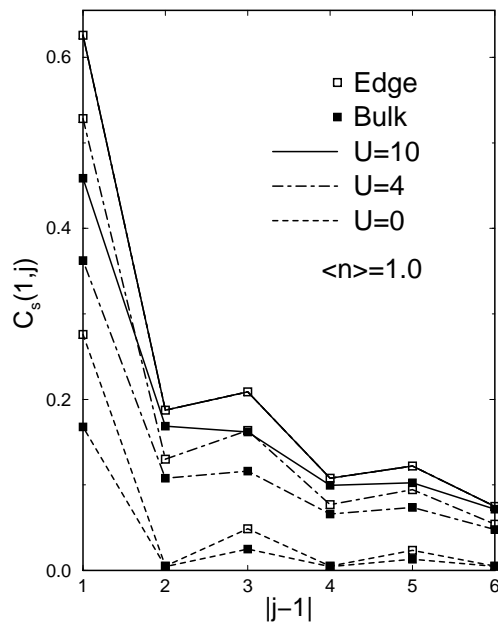


FIG. 9. $C_S(1, j)$ for the 1D Hubbard model using the DMRG technique on a 60 sites chain working at $\langle n \rangle = 1$ and the couplings shown ($t = 1$). The open (full) squares are results obtained locating site “1” next to the edge (at the center of the chain).

As U/t is reduced a smooth change in the spin correlations is observed. These correlations decrease in absolute value but the relative enhancement remains strong at short distances. The “zig-zag” pattern described in Sec.II is present even in the non-interacting limit $U/t = 0$. The example of the Hubbard model at weak coupling show us that the interpretation of the effect based on the RVB language of Sec.III may not be unique, and other explanations based on perturbative approaches in the small U/t limit could lead to similar conclusions. This is reminiscent of the presence of bulk strong antiferromagnetic correlations themselves which can be understood as a ground state property of a spin localized Heisenberg model, as well as arising from nesting properties of the half-filled noninteracting Hubbard model. In other words, $U/t = 0$ is a critical point for the one band Hubbard model with nearest-neighbor hopping and it already has strong indications of the existence of antiferromagnetic correlations in the ground state, although they are not of long range order.

Let us consider now the influence of density on the AF vacancy-induced enhancement. It is reasonable to expect that the effect will be observed as long as the bulk ground state spin correlations are dominantly staggered. Since previous experience with Hubbard-like models in 2D has shown that AF correlations are rapidly suppressed by doping [21], the same will likely occur with the AF enhancement near Zn -ions. Results at densities away from half-filling are presented in Fig.10 for $U/t = 4$.

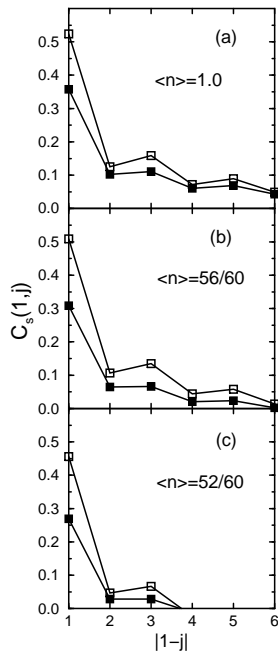


FIG. 10. $C_S(1, j)$ for the 1D Hubbard model using the DMRG technique on a 60 sites chain at $U/t = 4.0$ and the densities shown. The open (full) squares are results obtained locating site “1” next to the edge (at the center of the chain).

Indeed, the range of the AF correlations is certainly suppressed as $\langle n \rangle$ deviates just a small percent from half-filling. However, at very short distances such as 1,2, and 3 lattice spacings the effect remains visible. Specially the tendency to form a robust spin singlet between the two spins located the closest to the vacancy (or edge of an open chain) seems to survive the rapid reduction of the AF tail in the spin correlations. This result may have consequences for experimental investigations of the phenomenon investigated in this paper. For instance, in the normal state of underdoped cuprates, where it is believed that a AF correlation length of about a couple of lattice spacings should exist, Zn -doping may induce localized moments and small regions with nonzero staggered correlations. However, more work is needed to fully clarify the consequences of the vacancy-induced AF effect in cuprates since a combination of mobile charges and static defects may complicate the interpretation of experiments.

V. LOCAL SUSCEPTIBILITY

After studying in detail the equal-time spin correlations, in this section some experimental consequences of the vacancy-induced enhanced antiferromagnetism are described. The emphasis is given to NMR experiments where the measured spectra depends on the local spin susceptibility. The discussion here follows previous calculations in the context of the $S = 1/2$ Heisenberg chain where the theoretical predictions for the NMR spectra [17] have been recently confirmed experimentally [33].

A. Intuitive Expected Behavior:

The local susceptibility corresponding to site i and temperature T for any of the spin models used in Sec.II is defined as

$$\chi_i(T) = (1/T) \sum_j \langle S_i^z S_j^z \rangle, \quad (4)$$

in a standard notation. Note that as $T \rightarrow 0$ and working on a finite lattice, both the numerator and denominator vanish. The reason is that for spin systems of the family considered here the ground states are usually spin singlets which are separated from the excited states by a finite gap (which may be intrinsic to the model or caused by finite size effects). In such a situation $\sum_j S_j^z$ acting over the ground state produces a vanishing response. Then, in order to study the local susceptibility using the DMRG or Lanczos methods, which are zero temperature algorithms applied to finite clusters, the effect of a finite temperature needs to be simulated. For this purpose the first excited state in the energy spectrum having a finite spin (which typically is spin one or one-half depending on whether the number of sites is even or odd) will be used in Eq.(4) to obtain the $\langle \dots \rangle$ average. This state is

the first that contributes appreciably to the susceptibility when temperatures or magnetic fields of the order of the gap in the spectrum are considered, and here it will be denoted by $|\phi_S\rangle$ where S is 1 (1/2) for an even (odd) number of spins. Then, the low temperature local susceptibility used in the DMRG/Lanczos calculations below is redefined as

$$\chi_i \approx \sum_j \langle \phi_S | S_i^z S_j^z | \phi_S \rangle = S \langle \phi_S | S_i^z | \phi_S \rangle, \quad (5)$$

where in the last step the equality $\sum_j S_j^z | \phi_S \rangle = S | \phi_S \rangle$ was used. Comparing results using this approach with those of finite temperature Monte Carlo simulations presented later in the text, it will be shown that this definition captures not only qualitatively but even quantitative the important aspects of the low temperature behavior of the actual susceptibility $\chi_i(T)$ (for bulk gapless models this good agreement is expected for finite systems only i.e. when there is a small gap in the spectrum caused by size effects). Note also that the factor $1/T$ being just a multiplicative factor will simply be dropped from the calculations below, and thus the units in the reported local susceptibilities are arbitrary.

Let us discuss the expected qualitative behavior of χ_i as defined in Eq.(5) considering as example the spin correlations of a dimerized $J_1 - \delta$ model in the limit of a large enough δ (i.e. working in a ground state with a robust spin gap) such that the spins far from the chain edges mainly form tight spin singlets with their neighbor across the “strong” bonds of the chain. Let us also assume that the first link next to the edge is “weak”. In this situation it is intuitively reasonable (and Fig.3 confirms it) that the first two spins near the end will attempt to form a singlet at least part of the time. Fig.11a provides a snapshot of a typical spin configuration where a mismatch between the bulk spin singlet pattern and the spin singlet near the end can be observed.

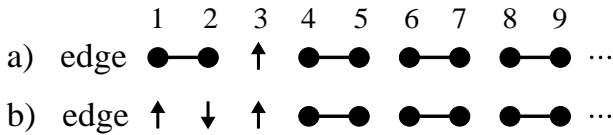


FIG. 11. (a-b) Two spin configurations relevant for the discussion on the development of a maximum in the local susceptibility close to an edge. See text for details.

At the location of the defect (which is a standard domain wall) a quasi-free spin 1/2 is located. It is clear that the local susceptibility for Fig.11a will have the value 1/4 at site 3 where the free spin is (since $\langle S_3^z S_{j \neq 3}^z \rangle = 0$), while at all other sites it will cancel since $\langle S_i^z S_i^z \rangle + \langle S_i^z S_{i+1}^z \rangle = 1/4 - 1/4 = 0$ (if i and $i+1$ are the locations of the spins forming a strong singlet) and $\langle S_i^z S_j^z \rangle = 0$ if $j \neq i+1$. Note, however, that the location of the free spin can certainly fluctuate when the full quantum mechanical calculation is carried out. In the case of the dimerized chain at hand, if the free spin has moved some distance away

from the vacancy the spins in between form the “wrong” vacuum i.e. they have the pattern of singlets on the weak links rather than the strong ones. This argument clearly shows that the free spin is localized near the chain end or vacancy, occupying a finite region of extension λ . It is reasonable to expect that the combination of configurations in the ground state of the localized spin (again, carrying out a full quantum calculation) will produce a spin susceptibility nonzero for $i < \lambda$ and approximately zero outside. Inside the bound state the spin configuration will be scrambled or disordered by the movement of the spin 1/2 defect, while outside it rigidly forms a dimerized pattern. In addition, it is also likely that the spin 1/2 may behave in the interval $1 \leq i \leq \lambda$ as a particle in a confining potential and, thus, its wave function will peak at a site away from the extremes. In this situation, χ_i will have a *maximum* at that particular site i inside $i < \lambda$. Finally, note that inside the bound state where the individual spins do not follow the same pattern as in the bulk, the antiferromagnetic nature of the Hamiltonian will induce an *alternation* in the sign of χ_i . As a toy model to understand this effect consider Fig.11b where near the edge 3 spins are considered to represent the $S = 1/2$ bound state, and the rest is forming very strong dimers. Solving exactly the 3 spin Heisenberg problem in the $S_{total}^z = 1/2$ subspace, the ground state has energy $-J$, the eigenvector is $|\psi_0\rangle = \sqrt{2/3}[|\uparrow\downarrow\uparrow\rangle - (1/2)(|\uparrow\uparrow\downarrow\rangle + |\downarrow\uparrow\uparrow\rangle)]$, and the spin correlations are $\langle S_1^z S_2^z \rangle = \langle S_2^z S_3^z \rangle = 1/6$ and $\langle S_1^z S_3^z \rangle = 1/12$ (the ground state can also be written as a combination of the state with a spin singlet between spins 1-2 and a spin up at 3, and the state with a spin singlet between spins 2-3 and a spin up at 1). The spin correlations produces susceptibilities $\chi_1 = \chi_3 = 1/6$ and $\chi_2 = -1/12$, showing the expected alternation. In other words, the spin at the center wants to point mostly down due to the influence of the two neighbors which are mainly up, and then the susceptibility has to be negative. $|\chi_i|$ is here maximized at the sites where the chances of having a spin up are the largest which are 1 and 3 (the 3 spin problem is too small to show a maximum away from the edges as it occurs on larger systems). A peak in χ_i away from $i = 1$ is expected for cases where λ is larger than 3 sites since spins at the center near $i \sim \lambda/2$ will be influenced by all the rest of the spins, while those near the end by only half of those spins.

Consider now a gapless system as a limit of a spin gapped model. It is intuitively plausible that as the spin gap of a given Hamiltonian is reduced, for instance by properly adjusting some couplings such as δ in the dimerized chain, the position of the maximum will move away from the chain end. In the limit where the gap vanishes, χ_i could become a monotonously growing function of distance i . This argument makes the results of Egger and Affleck [17] intuitively reasonable, although certainly do not replace the conformal field theory methods and Monte Carlo simulations employed by those authors. This expected behavior for gapless systems is observed in

the DMRG studies for the $S = 1/2$ Heisenberg model.

The local susceptibility is a symmetric function under reflexions with respect to the center of the chain studied, and it has rapid sign oscillations. Then, it can be separated into a “uniform” component χ_i^u and a “staggered” or “alternating” component using the definition $\chi_i = \chi_i^u - (-1)^i \chi_i^a$. Both of these components are now smooth functions of the site index. In practice the uniform part was obtained below using $\chi_i^u \approx \frac{1}{2}\chi_i + \frac{1}{4}(\chi_{i+1} + \chi_{i-1})$ and $\chi_i^a = -(-1)^i(\chi_i - \chi_i^u)$, where the former equation provides an approximate but accurate estimation of the uniform part for smooth functions of the site position. With these definitions the staggered component becomes an antisymmetric (symmetric) function of i for an even (odd) total number of sites (the proof is by simple explicit construction). In addition, it can be shown that as the chain size grows the sum $\sum_i \chi_i^u$ converges to the total spin in the z -direction of the state $|\phi_S\rangle$ considered in Eq.(5) (i.e. 1 (1/2) for an even (odd) number of sites). Then, $\chi_i^u \sim 1/N$ at the center of the chain if a gapless model is considered (i.e. the spin of the state is approximately uniformly distributed on the chain). For systems such as a dimerized lattice where a localized spin 1/2 appears near the ends of the chain and there is a spin gap, χ_i^u should vanish in the bulk of the chain and remain nonzero only at the ends. In the next subsections the qualitative expected behavior of χ_i discussed here will be tested using numerical techniques.

B. χ_i in the $S = 1/2$ Heisenberg chain

In Fig.12a the results for χ_i obtained with the DMRG method using a chain with 80 sites are shown (remember that the DMRG technique is applied with OBC i.e. it already simulates the presence of a couple of vacancies in the problem). The uniform and staggered components satisfy the expected behavior described before. As anticipated, χ_i^a initially grows with the distance i from the end of the chain as it should occur in the bulk [17]. However, Fig.12a and the previous discussion show that symmetry considerations force χ_i^a to vanish in the middle of the chain, changing sign between the left and right parts of the cluster, which is a finite size effect. The maximum in χ_i^a is located at a position slightly smaller than 1/4 of the chain length. Roughly, it is expected that the region between the first site $i = 1$ and the site where the maximum is obtained is representative of the bulk. Fig.12b shows again the two components of χ_i but now for a chain with an odd number of sites. Once again in agreement with the previous discussion now χ_i^a is symmetric.

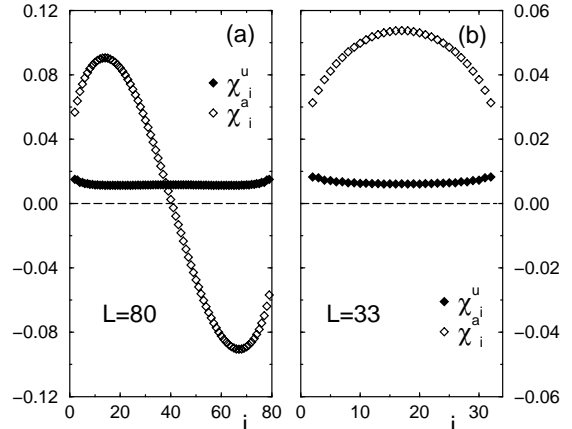


FIG. 12. Uniform and staggered components of the local susceptibility χ_i obtained with the DMRG method applied to the $S = 1/2$ Heisenberg model on a chain with L sites, using m states in the iterations and studying the subspace with a total spin in the z -direction equal to 1. (a) corresponds to $L = 80$ and $m = 16$, and (b) to $L = 33$ and $m = 32$.

It also grows away from the chain ends as for an even number of sites, but its maximum is reached in the middle of the chain. Then, the finite size effects are less severe in a chain with an odd number of sites. Fig.13 illustrates the expected behavior in the bulk analyzing short distances near the chain end using systems of length $N = 62, 80$ and 160.

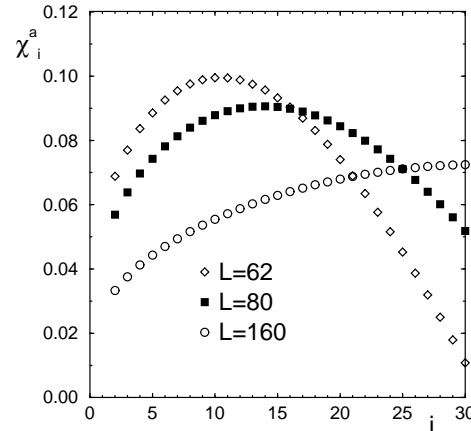


FIG. 13. Staggered component of χ_i for the $S = 1/2$ Heisenberg model on a chain, obtained with DMRG keeping $m = 16$ states. Results for several lengths are given.

The position of the maximum moves away from the chain end. For a long enough chain a monotonous increase of χ_i^a is recovered in agreement with the calculations of Eggert and Affleck [17].

C. χ_i in the frustrated $S = 1/2$ Heisenberg chain

Fig.14a,b contain results similar to those of Fig.12a,b but now introducing frustration in the Hamiltonian using a Heisenberg interaction at distance of two lattice spacings regulated by the coupling J_2 . For the particular case $J_2/J_1 = 0.5$ the ground state is known to consist of spin dimers at alternating links, and it has a spin-gap (on a finite chain with PBC, it is doubly degenerate) [29]. In spite of such clear differences between the ground states at $J_2/J_1 = 0$ and 0.5, the local susceptibility behaves very similarly as shown in the figure. The uniform component does not show any sign of having a localized spin state near the ends (actually the spin distribution has its minimum at the edges). Then, the spin $J_1 - J_2$ model has a finite spin gap and yet no localized spin $1/2$ states near the edges. A very similar behavior was observed in the case $J_2/J_1 = 0.4$ (not shown), and, thus, the results of Fig.14a,b can be considered as representative of the spin gapped regime of the frustrated Heisenberg chain. An enhanced staggered susceptibility does not only exist in the unfrustrated Heisenberg model but also in a much broader family of models that include frustration in the Hamiltonian. The key common ingredient to obtain quantitatively a growing χ_i away from the edges seems the absence of localized spins at the ends. Thus it is here concluded that the phenomenon of a growing staggered susceptibility at zero temperature away from the edges is more general than previously expected.

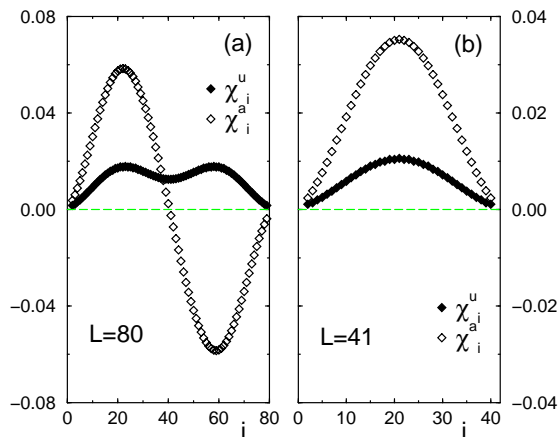


FIG. 14. Uniform and staggered components of the local susceptibility χ_i obtained with the DMRG method applied to the frustrated $S = 1/2$ Heisenberg model with $J_2/J_1 = 0.5$ on a chain with L sites, using m states in the iterations and studying the subspace with a total spin in the z -direction equal to 1. (a) corresponds to $L = 80$ and $m = 32$, and (b) to $L = 41$ and $m = 32$.

Here it is important to remark that the behavior described in this subsection could actually be observed in spin-Peierls systems such as CuGeO_3 . To understand this statement note that the similarities between the re-

sults of subsections V.B and V.C are caused by the dynamical adjustment in the latter of the pattern of spin dimers that appear at $J_2/J_1 = 0.5$. When a vacancy breaks a spin singlet, the local “damage” is avoided by a dynamical process similar to the one discussed in Fig.7. For an even number of sites between vacancies this effect heals completely the damage (while with an odd number of sites a soliton appears at mid-distance between the vacancies). Thus, there are no spin- $1/2$ states localized near the Zn -vacancies. A similar process is expected to occur in spin-Peierls systems where the phonons are dynamical variables which can also adjust the pattern of strong and weak links. Preliminary Monte Carlo numerical results show that this effect indeed occurs in practice [34].

D. χ_i in the dimerized Heisenberg chain

The behavior for the case of a dimerized $J_1 - J_2 - \delta$ spin chain is quantitatively very different from that observed in the $S = 1/2$ Heisenberg model with and without frustration, although qualitatively they are related. Fig.15 shows results for a representative value of the dimerization $\delta = 0.048$ [35]. The first and last links are “weak” in Fig.15. Here χ_i^u is nonzero only in the neighborhood of $i = 1$ and $i = N$. By symmetry the spin near each end is $1/2$, since the total spin is 1 for an even number of sites in the cluster. It is important to note that the staggered component is also localized in approximately the same range as the uniform one since the bulk susceptibility must vanish. These results coexist with a spin-spin enhancement of the static correlations which are also concentrated on a finite region near the ends (Sec.II).

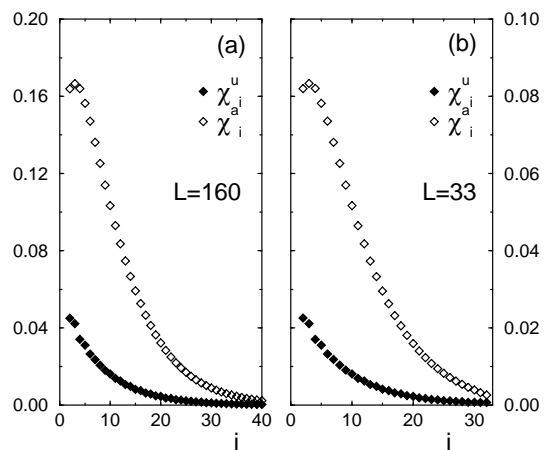


FIG. 15. Uniform and staggered components of the local susceptibility χ_i obtained with the DMRG method applied to the dimerized $S = 1/2$ chain with no frustration $J_2/J_1 = 0$ and $\delta = 0.048$ on a chain with L sites, using m states in the iterations and studying the subspace with a total spin in the z -direction equal to 1. (a) corresponds to $L = 160$ and $m = 20$, and (b) to $L = 33$ and $m = 32$. In both cases the first link after the left chain end is “weak”.

The absence of spin-charge separation produces virtually negligible size effects in the figure which is manifest in the vanishing of both components at distances from the edges approximately larger than 40. This has to be contrasted with Fig.13 for the undimerized case where the staggered component changed appreciably with the lattice size moving the location of its maximum away from the edge. In the dimerized case and for the parameter δ used here, the maximum is at two lattice spacings from the chain end and remains there as the clusters grow. Again, all this is a simple manifestation of the different localized vs delocalized character of the spin at the edges for dimerized and undimerized chains, respectively. Fig.15b contains results for an odd number of sites $L = 33$. With only a total spin $1/2$ to be distributed the chain selects one end as the depository of such spin and leaves the other spinless. This depends on whether the first link on the chain, say starting from the left, is weak or strong (the weak link carries the localized spin). Finally, note that if the first and last links would have been “strong” then there is no reason for having a localized spin $1/2$ near the end. In this situation the spin is expected to be delocalized with a maximum probability of being located near the center of the chain (as illustrated below in Fig.16b).

Combining frustration and dimerization ($J_2/J_1 = 0.35$ and $\delta = 0.012$) gives results similar to those of Fig.15. The localization length is only slightly larger than for the case $J_2/J_1 = 0$, $\delta = 0.048$. Now the maximum in the staggered component is at site $i = 5$ which also reflects on a larger extension of the region where the spin-spin correlations are perturbed with respect to their bulk behavior by the influence of the chain ends.

Note that for a short chain of e.g. 20 sites, the staggered susceptibility would behave very similarly to the results for the unfrustrated undimerized case Fig.12a. It is clear that if the spin localization length is similar to the length of the chain (which mimics the distance between Zn impurities in real systems) then the spin and charge are deconfined. Also the qualitative trend of having a smaller disturbance in size near the ends as δ grows can be shown in the extreme case of a large dimerization such as $J_2/J_1 = 0$, $\delta = 0.5$ (Fig.16a). Here the staggered susceptibility reaches its maximum at $i = 1$ i.e. in the first site of the chain, and the uniform component is localized within 3 or 4 lattice spacings of the chain end.

Finally, in Fig.16b results are presented for the case $J_2/J_1 = 0.35$ and $\delta = 0.012$ treated before, but now with the first and last links being “strong”. The uniform susceptibility suggests that the spin is not localized at the ends but it lives mainly near the center as it occurs for a free particle in a square-well potential. This agrees with the previous discussion where it was argued that in a dimerized chain the $S = 1/2$ near Zn appears only on one side of the vacancy, the one with the weak link immediately next to Zn . Thus, qualitatively the results are as in the case of spin-charge separation discussed before, and the staggered susceptibility has a behavior similar

to that of Fig.12a for the $S = 1/2$ Heisenberg chain. Thus, assuming that Zn doping simply produces severed chains that keep their pattern of weak and strong bonds (frozen phonons), there will be segments with even sites where the spins are both either localized or delocalized, depending on whether the first link is weak or strong, and also segments with an odd number of sites where there is always one localized spin. The latter was illustrated in Fig.12.b for the case of a $L = 33$ chain.

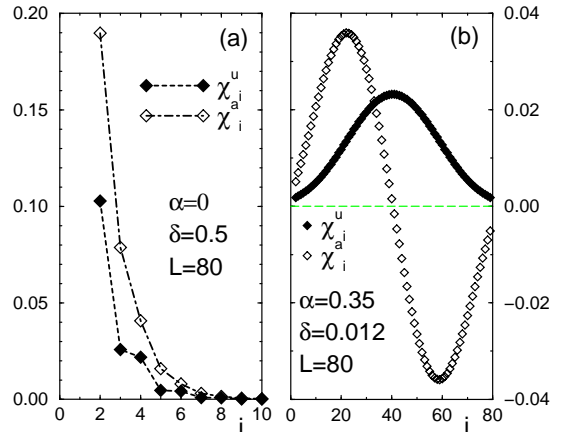


FIG. 16. Uniform and staggered components of the local susceptibility χ_i obtained with the DMRG method applied to the dimerized $S = 1/2$ chain with frustration on a chain with L sites, using m states in the iterations and studying the subspace of total spin z -projection 1. (a) corresponds to $\delta = 0.5$, $J_2/J_1 = 0.0$, $L = 160$ and $m = 20$, with the first links being “weak”, and (b) has $\delta = 0.012$, $J_2/J_1 = 0.35$, $L = 80$ and $m = 32$ with the first links being “strong”.

Once again note that our discussion of subsection V.C suggests that in the case of a compound where the coupling of spins and lattice is dynamical, such as in the spin-Peierls systems, the pattern of strong and weak links adjusts such that the first and last links are always strong in a given chain segment with an even number of sites. Thus, the results of Fig.16b are relevant for this type of compounds.

E. χ_i in a Heisenberg ladder cluster

Similar calculations can be carried out for ladder systems. In Fig.17 results for the full local susceptibility χ_i are given for a ladder with 2×32 sites and vacancies located at rung 11 and 22 in the same sublattice (two impurities are introduced to produce an integer total spin). For the case of no impurities, the susceptibility (which is entirely “uniform”) does not have structure showing that the ends of the ladder do not localize spin (remember that open boundary conditions are used in the DMRG method). On the other hand, when the vacancies are introduced a clear enhancement in χ_i is observed which is

correlated with the position of the vacancy in, e.g., rung 11. The maximum change is always in the site located in

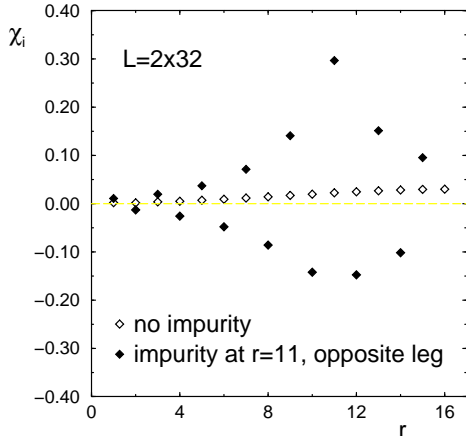


FIG. 17. Local susceptibility for the Heisenberg model on a 2×32 ladder using DMRG, keeping $m = 16$ states, and studying the state of lowest energy in the subspace of total spin in the z -direction equal to 1. Results with and without impurities are shown, in the former running along the opposite leg from those impurities which are located at rungs 11 and 22.

front of the vacancy along the same rung. Fig.18a,b show the uniform and alternating components.

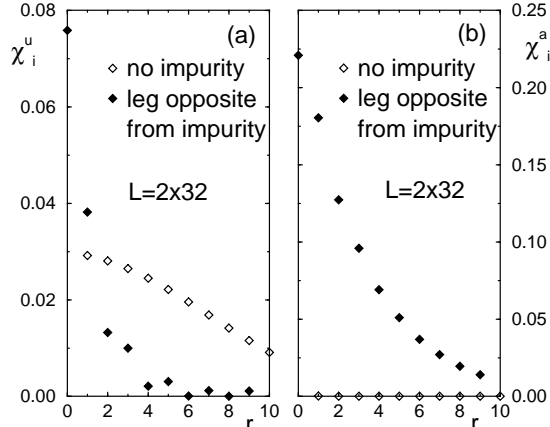


FIG. 18. Local susceptibility for the Heisenberg model on a 2×32 ladder using DMRG, keeping $m = 16$ states, and studying the state of lowest energy in the subspace of total spin in the z -direction equal to 1. Results with and without vacancies are shown. (a) contains the uniform component and (b) the staggered one.

The localization length for the $S = 1/2$ seems of about 2 to 3 lattice spacings (as previously noticed by Sandvik et al. [30]). Then, ladders and dimerized chains both behave very similarly presenting localized $S = 1/2$ states near vacancies and an enhanced staggered susceptibility in their vicinity. On the other hand, the Heisenberg

model with and without frustration has no localized spins near vacancies and a staggered susceptibility that grows with the distance from the vacancy. In spite of these differences, below it is argued working at finite temperatures and/or high concentration of vacancies both families of models should present qualitatively similar behavior that can be observed experimentally using NMR techniques.

VI. MONTE CARLO RESULTS FOR DIMERIZED CHAINS

To study the temperature dependence of some of the results shown in previous sections, a standard world-line Monte Carlo simulation of the dimerized unfrustrated ($\delta \neq 0$, $J_2/J_1 = 0$) Heisenberg model on a chain was performed. The limitation of having $J_2/J_1 = 0$ is technical: the addition of frustration would have spoiled the simulation due to the appearance of a “sign problem”. Results for the case of a $L = 80$ chain, open boundary conditions, $\delta = 0.05$, and with “weak” first and last links are shown in Fig.19a,b (to collect good statistics about 3 to 4 independent runs with 10^6 sweeps each were carried out. The maximum number of Trotter slices used was 120). The behavior of the uniform susceptibility near the end is particularly interesting. It shows the development of the spin $1/2$ bound state as the temperature is reduced, in excellent agreement with the DMRG and Lanczos results. The crossover from a localized to delocalized spin $1/2$ occurs roughly near $T^* \sim 0.1J$, and this should be a temperature of relevance in the experimental study of materials with structural dimerization. The staggered component follows a similar pattern.

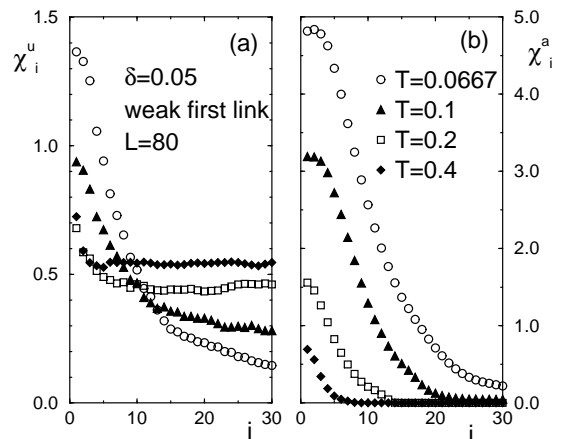


FIG. 19. Staggered susceptibility for the dimerized spin model obtained with Monte Carlo techniques on a chain with 80 sites and OBC. The temperatures and δ are shown. (a) contains the uniform component while (b) has the staggered one. The distribution of dimerized links is such that the first link on the chain immediately after the edge is “weak” (thus, generating a spin $1/2$ localized state in its vicinity at very low temperature).

Fig.20.a,b illustrates what occurs in the case where the first and last links are “strong”. As discussed before no localized states are expected in this situation and indeed the uniform susceptibility has no structure near the end of the chain even at low temperatures. Nevertheless it is curious that the staggered component shows structure at intermediate temperatures, although their intensity is much smaller than for the case of “weak” links at the ends.

Finally, for completeness in Fig.21a,b results for the pure $S = 1/2$ unfrustrated undimerized Heisenberg model are shown to compare Monte Carlo predictions with the DMRG results of Fig.12.

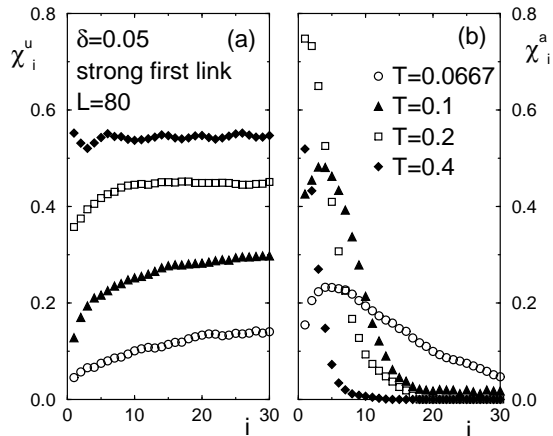


FIG. 20. Same as Fig.19 but now with a “strong” first link. In this situation there are no localized spin 1/2 states near the edges.

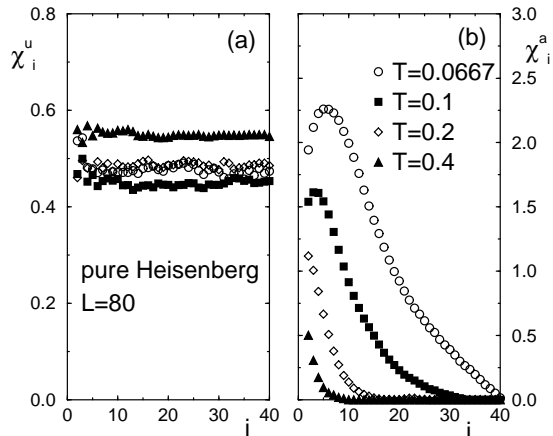


FIG. 21. Staggered susceptibility for the spin 1/2 Heisenberg chain obtained with Monte Carlo techniques on a 80 sites chain and using OBC. Data for different temperatures are shown. (a) contains the uniform component, while (b) has the staggered one.

The uniform component has no structure as expected,

while the staggered one develops a strong peak which grows in intensity and moves the location of its maximum away from the edge as the temperature is reduced, in qualitative agreement with Fig.12. Fig.22 contains results using the Monte Carlo approach, with and without constraining the simulation to the subspace with a total z -component of the spin equal to 1, and DMRG results in the lowest energy state of total z -component spin 1, as used in most of Sec.V.

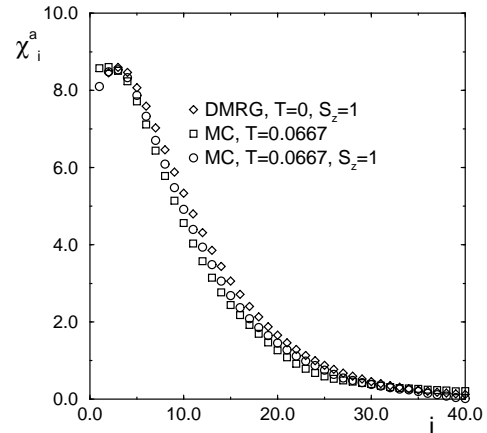


FIG. 22. Staggered susceptibility for the dimerized spin model obtained using different techniques. The DMRG results were calculated on a 160 sites chain with $\delta = 0.048$, and a total z -component of the spin in the ground state equal to 1. The Monte Carlo (MC) results were calculated on chains with 80 sites and $\delta = 0.05$. In one case the total z -component of the spin was fixed to 1, and in the other not. The distribution of dimerized links is such that the first link on the chain immediately after the edge is “weak”. The amplitudes have been adjusted such that the maxima have the same height. The agreement between the different curves suggests that the methods of calculation used in this paper are equivalent at low temperatures.

The excellent agreement between all the results show that the three methods are quantitatively equivalent at low temperatures. Similar results have been obtained in the context of the 2-leg and 3-leg ladders by Sandvik et al. [30].

VII. PREDICTIONS FOR THE NMR SPECTRUM

As explained in the introduction, previous calculations in the context of the $S = 1/2$ Heisenberg chain showing that the local susceptibility near a chain edge has a large alternating component led to interesting predictions for the temperature dependence of some NMR experiments [17]. More specifically, the alternating staggered magnetization that such a local susceptibility would produce in the presence of a magnetic field can be detected as a broadening of the NMR spectra. These predictions

have been recently summarized and verified experimentally by Takigawa et al. [33]. Let us denote as K_i the shift at site i of the resonance field induced by the hyperfine interaction between nuclear and electron spins. The NMR spectrum simply represents the distribution function of K_i 's. However, it can be shown [33] that apart from a uniform shift, K_i is proportional to χ_i^a . Actually ^{63}Cu NMR experiments carried out in Sr_2CuO_3 , a compound with dominant one dimensional structures presumably well described by the $S = 1/2$ Heisenberg model, have provided results compatible with the theoretical predictions [33].

The previous discussion shows that the distribution of the local susceptibility or its staggered component provides interesting information for NMR experiments. This information can be easily obtained from the results of Sec.V. The qualitative discussion presented in this paper shows that the effect observed before for the $S = 1/2$ Heisenberg model [17] is a particular case of a more general situation. Our analysis predicts that if materials can be found that are a physical realization of frustrated $S = 1/2$ Heisenberg models ($J_2/J_1 \neq 0$) they would present NMR spectra very similar to those of Sr_2CuO_3 . In addition, spin-Peierls systems may also have a NMR spectra similar to that of undimerized chains since phonons can adjust dynamically the pattern of strong and weak links, avoiding the presence of localized spin-1/2 states near vacancies.

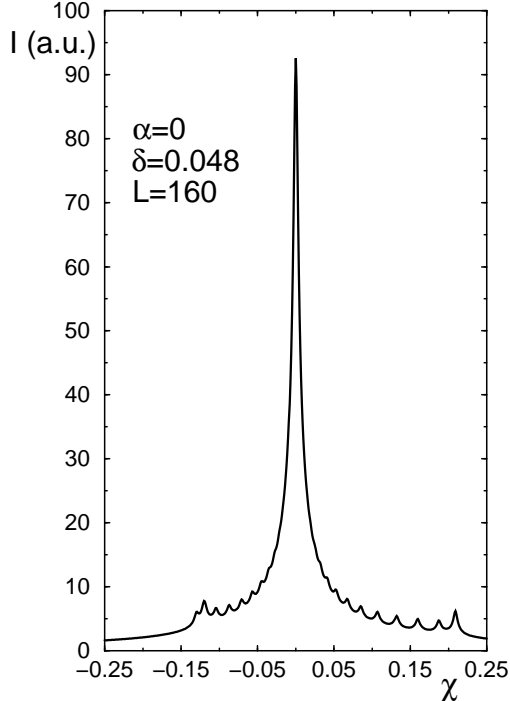


FIG. 23. NMR spectra for a dimerized chain with $\delta = 0.048$ using a “weak” first link on the chain and the DMRG technique (keeping $m = 20$ states).

In addition, nontrivial results can be obtained also for structurally dimerized chains, such as $\text{Cu}(\text{NO}_3)_2 \cdot 2.5\text{H}_2\text{O}$, CuWO_4 , $(\text{VO})_2\text{P}_2\text{O}_7$, and $\text{Sr}_{14}\text{Cu}_{24}\text{O}_{41}$. In this case the local susceptibility does *not* grow with distance at zero temperature due to the fact that there is no spin-charge separation in the system, i.e. a spin 1/2 is localized near the chain ends. Nevertheless, a broadening in the overall NMR spectra is predicted as the temperature dependence of the Monte Carlo results in Fig.19 suggests. In this case, since the magnetic susceptibility in the bulk is zero, the distribution of χ_i will be centered at zero. As T is reduced the maximum value of $|\chi_i|$, related with the total width of the NMR spectra, moves away from the chain end, as the MC results of Fig.19b imply. The central peak must increase its width as the temperature is reduced.

Results for the distribution of χ 's obtained with DMRG techniques at zero temperature but, as discussed before, in the total spin projection $S_z = 1$ subspace are presented in Fig.23. They qualitatively agree with the results of the Monte Carlo simulations at the lowest temperature available. The actual temperature dependence of these MC results is given in Fig.24.

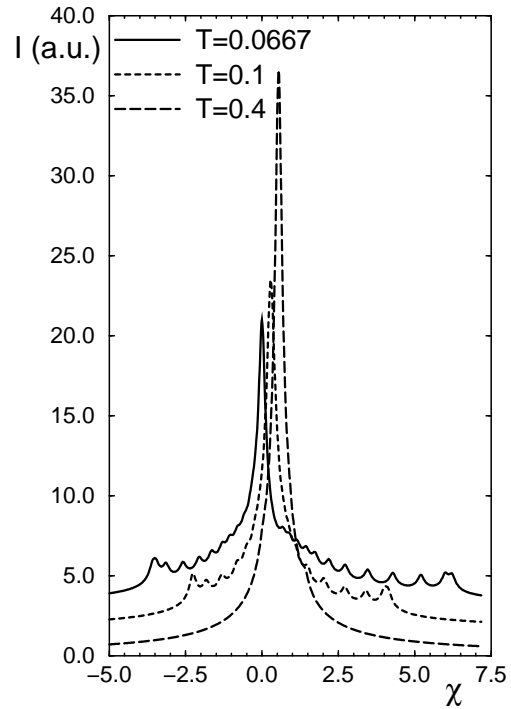


FIG. 24. Same as Fig.23 but now calculated with Monte Carlo simulations at different temperatures (in units of J) using the results of Fig.19. The broadening of the shoulder with lower temperatures reflects the increase of the local susceptibility at the boundaries. The shift of the main peak with increasing temperature is due to the increased “bulk” susceptibility.

Fig.25a contains DMRG results for $J_2/J_1 = 0.35$ and

$\delta = 0.012$. In this case Monte Carlo simulations cannot be performed due to technical reasons (sign problems). Nevertheless, the DMRG result is qualitatively similar to those in Fig.23. The NMR spectra contained in Figs.23-25a are predictions of our calculations that could be checked experimentally to address the universality of the staggered susceptibility enhancement near chain ends described in this paper. Qualitatively the predictions are similar as reported by Sandvik et al. [30] in the context of the 2-leg and 3-leg spin ladders.

Note that the results of Fig.25, as well as the previous NMR calculations [17], have been performed on a single chain of length L , with L large. These results can only be applied to real systems with a very low concentration of impurities. Actually the experiments in Sr_2CuO_3 [33] were carried out without adding explicit doping but simply expecting the spontaneous presence of a finite (and very small) concentration of vacancies in the system. In the same spirit, experiments in structurally dimerized chains or spin-Peierls systems can be conducted also without Zn doping, and the results should be close to those discussed in Figs.23 and 25b.

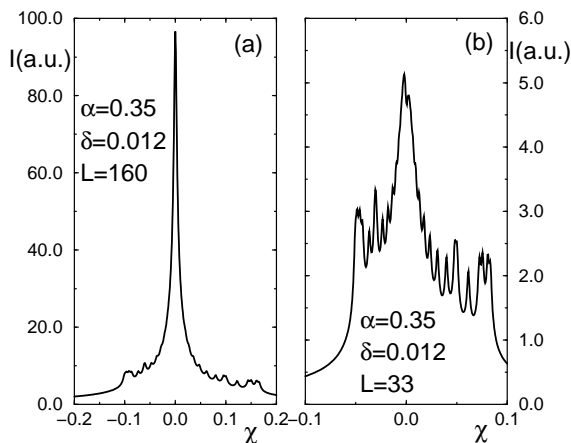


FIG. 25. (a) Same as Fig.23 but using $J_2/J_1 = 0.35$, and $\delta = 0.012$; (b) NMR spectra for the case of a “short” chain of 33 sites. $m = 32$ states were kept in the DMRG technique.

However, for completeness, here results for short chains are also shown to mimic the behavior of structurally dimerized compounds explicitly doped by Zn . For instance, if the length of the chain is $L = 33$, then the results should be contrasted with Zn -doped $x \sim 0.03$. A representative result is shown in Fig.25b. Note that now the central peak is much broader than in Fig.25a, and the background has comparably much more intensity. Results for even shorter chains reveal the discrete nature of the chain, presenting just a small number of peaks in the histogram. However, in a real system the Zn impurities will not lie uniformly distributed at distance $l \sim 1/x$, but they will follow a random pattern producing a distribution of chain lengths that includes short and long ones. (Fig.26 shows explicitly the distribution

of distances between two impurities). Thus, it is reasonable to expect experimentally a mixing of results such as those of Figs.25a and 25b for Zn -doped compounds. In spite of these complications, for small values of x clearly a large central peak will appear as a dominant structure on top of a background that increases its size (without diverging for dimerized systems) as the temperature is reduced.

Very recently NMR spectra for Zn -doped $SrCu_2O_3$, which is a spin ladder system, has been presented [36]. The results show a large broadening of the main signal in the NMR spectra as the temperature is reduced from 280K to 20K for the case of a Zn concentration of just 0.25% and 0.50%.

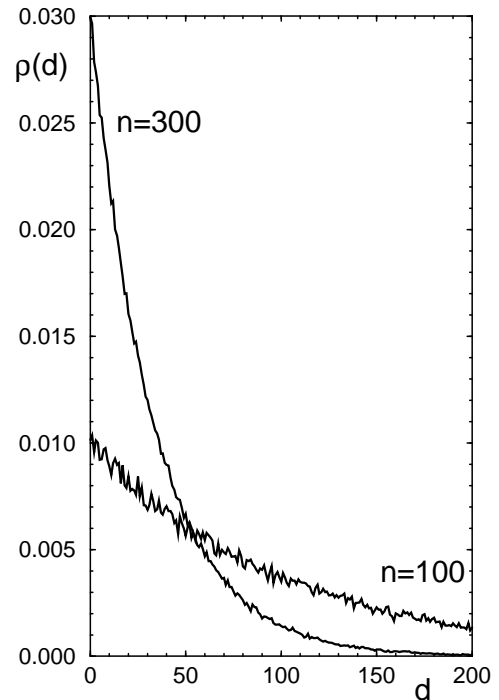


FIG. 26. Distribution of distances d between two impurities working on a chain of length 10,000 sites, with n impurities randomly distributed. Each curve is an average over 1,000 distributions of impurities.

The authors conclude that a picture where each doped vacancy induces a spin $1/2$ localized in the same rung as the vacancy cannot explain this result since the vast majority of the spins would be unaffected by doping. This conclusion is in excellent agreement with the observation throughout this paper that for realistic values of parameters the region in the vicinity of the vacancies where the staggered local susceptibility is enhanced can be large, involving several lattice spacings. For ladders Fig.18 suggest that in this case ~ 10 rungs (i.e. 20 sites) away from the vacancy still have enhanced antiferromagnetism. If a 2-leg ladder with 2×100 sites and open BC is considered (to mimic the undoped ladder segments for

a nominal Zn -concentration of 0.5%), then 20% of the system is affected by the edges. In addition, the extra broadening effect caused by the probabilistic existence of short segments (see Fig.26) should in principle be taken into account to contrast theory with experiments. This detailed calculation will be carried out in future publications, but here it is safe to conclude that the recent NMR spectra in ladder systems is compatible with the results presented in this paper.

VIII. CONCLUSIONS

The effect of vacancies on a variety of spin models and geometries has been studied with the help of computational techniques. Near these vacancies the staggered spin-spin correlations are clearly enhanced. The range of the effect can vary from just a few lattice spacings (for strongly dimerized systems or models with large spin gaps where a spin $1/2$ state is bounded to the chain edge) to the whole lattice (for the $S = 1/2$ Heisenberg model with and without frustration where there is no spin $1/2$ bound state near the vacancies). The origin of this phenomenon was here described in terms of short-range RVB states. Introducing vacancies prunes or reduces the number of possible spin singlet configurations and this enlarges the spin correlations as described in this paper. The phenomenon also takes place in 2D models, although the effect here is not as large as in 1D. The AF enhancement can be observed in the behavior of NMR experiments as a broadening of the spectra as the temperature is reduced in structurally dimerized chains, ladders such as $SrCu_2O_3$, spin-Peierls compounds, and other materials after Zn impurities are introduced. In addition, it is likely that the enlarged AF correlations can stabilize 3D Néel order upon Zn doping once a weak correlation between chains and ladders is incorporated, in agreement with experimental results [4,5].

IX. ACKNOWLEDGMENTS

M.L. and E.D. are supported by grant NSF-DMR-9520776. G.B.M. acknowledges the financial support of the Conselho Nacional de Desenvolvimento Científico e Tecnológico (CNPq-Brazil). C. J. G. acknowledges the financial support of the Consejo Nacional de Investigaciones Científicas y Técnicas (CONICET-Argentina). Additional support by the National High Magnetic Field Lab is acknowledged.

- [2] M. Azuma, Z. Hiroi, M. Takano, K. Ishida, Y. Kitaoka, Phys. Rev. Lett. **73**, 3463 (1994); D. C. Johnston et al., Phys. Rev. **B35**, 219 (1987).
- [3] M. Uehara, T. Nagata, J. Akimitsu, H. Takahashi, N. Mori, and K. Kinoshita, J. Phys. Soc. Jpn. **65**, 2764 (1996).
- [4] M. Azuma, Y. Fujishiro, M. Takano, T. Ishida, K. Okuda, M. Nohara, and H. Takagi, Phys. Rev. **B 55**, R8658 (1997); M. Nohara, H. Takagi, M. Azuma, Y. Fujishiro, and M. Takano, preprint.
- [5] M. Hase, et al. Phys. Rev. Lett. **70**, 3651 (1993); S. B. Oseroff, et al., Phys. Rev. Lett. **74**, 1450 (1995); M. Hase, et al., Physica B **215**, 164 (1995).; J. G. Lussier, et al., J. Phys. Cond. Matt. **7**, L325 (1995); L. P. Regnault, et al., Europhys. Lett. **32**, 579 (1995); J.-P. Renard, et al., Europh. Lett., **30**, 475 (1995).
- [6] See J. C. Bonner, S. A. Friedberg, H. Kobayashi, D. L. Meier, and H. W. J. Blöte, Phys. Rev. B **27**, 248 (1983), and references therein.
- [7] B. Lake, D. A. Tennant, R. A. Cowley, J. D. Axe, and C. K. Chen, J. Phys. Cond. Mat. **8**, 8613 (1996), and references therein.
- [8] A. W. Garrett, S. E. Nagler, D. A. Tennant, B. C. Sales, and T. Barnes, Phys. Rev. Lett **79**, 745 (1997).
- [9] Z. Hiroi, S. Amelinckx, G. Van Tendeloo, and N. Kobayashi, Phys. Rev. B **54**, 15849 (1996).
- [10] G. B. Martins, E. Dagotto, and J. Riera, Phys. Rev. **B 54**, 16032 (1996).
- [11] Y. Motome, N. Katoh, N. Furukawa, and M. Imada, J. Phys. Soc. Jpn. **65**, 1949 (1996); M. Sigrist and A. Furusaki, J. Phys. Soc. Jpn. **65**, 2385 (1996); H.-J. Mikeska, U. Neugebauer, and U. Schollwöck, preprint cond-mat/9608100; T. K. Ng, Phys. Rev. **B 54**, 11921 (1996); T. K. Ng, preprint cond-mat/9610016; Y. Iino and M. Imada, J. Phys. Soc. Jpn. **65**, 3728 (1996); M. Imada and Y. Iino, J. Phys. Soc. Jpn. **65**, 568 (1997); K. Hida, preprint cond-mat/9612232; T. Miyazaki, M. Troyer, M. Ogata, K. Ueda, and D. Yoshioka, preprint cond-mat/9706123; M. Fabrizio and R. Mélin, preprint cond-mat/9703102; and references therein.
- [12] H. Fukuyama, T. Tanimoto, and M. Saito, J. Phys. Soc. Jpn. **65**, 1183 (1996); H. Fukuyama, N. Nagaosa, M. Saito, and T. Tanimoto, J. Phys. Soc. Jpn. **65**, 2377 (1996); N. Nagaosa, A. Furusaki, M. Sigrist, and H. Fukuyama, J. Phys. Soc. Jpn. **65**, 3724 (1996).
- [13] M. Azuma, M. Takano, and R. S. Eccleston, preprint cond-mat/9706170. See also M. C. Martin, M. Hase, K. Hirota, G. Shirane, Y. Sasago, N. Koide, and K. Uchinokura, preprint.
- [14] P. Lemmens, M. Fisher, G. Güntherodt, C. Gros, P. G. J. van Dongen, M. Weiden, W. Richter, C. Geibel, and F. Steglich, preprint cond-mat/9703060.
- [15] A. K. Hassan, L. A. Pardi, G. B. Martins, G. Cao, and L. C. Brunel, preprint cond-mat/9706286.
- [16] S. Miyashita and S. Yamamoto, Phys. Rev. **B 48**, 913 (1993); Erik Sorensen and Ian Affleck, Phys. Rev. **B 49**, 15771 (1994); and references therein. See also I. Affleck et al., Phys. Rev. Lett. **59**, 799 (1987).
- [17] S. Eggert and I. Affleck, Phys. Rev. Lett. **75**, 934 (1995); S. Eggert and I. Affleck, Phys. Rev. **B 46**, 10866 (1992).

[1] For a recent review see E. Dagotto and T. M. Rice, Science **271**, 618 (1996).

- [18] N. Bulut et al., Phys. Rev. Lett. **62**, 2192 (1989).
- [19] G. B. Martins, M. Laukamp, J. Riera, and E. Dagotto, Phys. Rev. Lett. **78**, 3563 (1997).
- [20] P. W. Anderson, Mater. Res. Bull. **8**, 153 (1973).
- [21] E. Dagotto, Rev. Mod. Phys. **66**, 763 (1994).
- [22] S. R. White, Phys. Rev. Lett. **69**, 2863 (1992).
- [23] H. Frahm and A.A. Zvyagin, ITP-UH-19/97, preprint.
- [24] J. Riera and A. Dobry, Phys. Rev. B **51**, 16098 (1995), and references therein.
- [25] E. Dagotto, and A. Moreo, Phys. Rev. Lett. **63**, 2148 (1989); and references therein.
- [26] J. Deisz, Phys. Rev. B **46**, 2885 (1992), and references therein.
- [27] S.A. Kivelson, D.S. Rokhsar, and J.P. Sethna, Phys. Rev. B **35**, 8865 (1987).
- [28] E. Dagotto and A. Moreo, Phys. Rev. B **38**, 5087 (1988) and references therein.
- [29] C. K. Majumdar and D. K. Ghosh, J. Math. Phys. **10**, 1388 (1969).
- [30] A. Sandvik, E. Dagotto, and D. Scalapino, preprint.
- [31] Actually the 1-2 singlet is more probable than 1-3 and 1-4 due to the characteristics of the 2-leg ladder ground state [1]. This detail is not qualitatively relevant here.
- [32] Recent work has addressed the special case of impurities in the form of $U = 0$ centers. Enhanced AF correlations were observed. See M. Ulmke, P. J. H. Denteneer, R. T. Scalettar, and G. T. Zimanyi, preprint, cond-mat/9707068.
- [33] M. Takigawa, N. Motoyama, H. Eisaki, and S. Uchida, Phys. Rev. B **55**, 14129 (1997).
- [34] J. Riera et al., in preparation.
- [35] Note that this number is selected since it was mentioned before in the phenomenological description of NaV_2O_5 (see D. Augier, D. Poilblanc, S. Haas, A. Delia, and E. Dagotto, Phys. Rev. B **56**, R5732 (1997)). However, the discussion of subsection V.C implies that a spin-Peierls system may be better described by the results of Fig.14, rather than those for a rigidly dimerized compound.
- [36] N. Fujiwara, H. Yasuoka, Y. Fujishiro, M. Azuma, and M. Takano, preprint.